A dynamic subgrid-scale model for LES of the G-equation

By A. Bourlioux[1], H. G. Im[2] and J. H. Ferziger[3]

1. Introduction

Turbulent combustion is a difficult subject as it must deal with all of the issues found in both turbulence and combustion. (We consider only premixed flames in this paper, but some of the ideas can be applied to the non-premixed case.) As in many other fields, there are two limiting cases that are easier to deal with than the general case. These are the situations in which the chemical time scale is either much shorter or much longer than the time scale associated with the turbulence. We deal with the former case. In this limit, the flame is thin compared to the turbulence length scales and can be idealized as an infinitely thin sheet. This is commonly called the flamelet regime; it has been the subject of many papers and the basis for many models (see, *e.g.*, Liñán & Williams 1993).

In the flamelet model, the local flame structure is assumed to be identical to the laminar flame structure; thus the flame propagates normal to itself at the laminar flame speed, S_L. This allows the use of simple approximations. For example, one expects the rate of consumption of fuel to be proportional to the area of the flame surface. This idea allowed Damköhler (1940) to propose that the wrinkled flame could be replaced by a smooth one which travels at the turbulent flame speed, S_T, defined by

$$S_T/S_L = A_L/A_p \tag{1}$$

where A_L is the total flame surface area and A_p is the area projected onto the mean direction of propagation. This relation can be expected to be valid when the flame structure is modified only slightly by the turbulence. A measure of the degree of modification is the Karlovitz number, Ka; Eq. (1) should hold when this parameter is not too large.

More recent approaches have attempted to relate the turbulent flame speed to turbulence intensity, u', which, presumably, characterizes the wrinkling of the flame. These result in relationships that typically take the form:

$$S_T/S_L = 1 + C(u'/S_L)^\alpha. \tag{2}$$

For the turbulent flow dominated by an inertial range, Pocheau (1992) derived a linear relation (Eq. (2) with $\alpha = 1$). Earlier work (Clavin & Williams 1979) also

1 CERCA, Université de Montréal
2 Center for Turbulence Research
3 Stanford University

predicted linear behavior in the limit of high turbulence intensity; other authors have produced theories that give different exponents (Yakhot 1988, Kerstein & Ashurst 1992). In §3, we shall use DNS to demonstrate that the linear relation is valid, at least in the limit appropriate to LES; we shall use the database of Trouvé & Poinsot (1994) and the zero heat-release data of Im (1996).

2. Large eddy simulation based on the G-equation

The above ideas can be applied to modeling the small scales of the wrinkling and thus produce the basis for large eddy simulation. It can be shown that a surface that moves at speed S_L normal to itself in a moving fluid can be represented as a level surface of the G-equation (Kerstein et al. 1988):

$$\frac{\partial G}{\partial t} + \frac{\partial}{\partial x_j}(u_j G) = S_L |\nabla G|. \tag{3}$$

To perform large-eddy simulation, the G-equation is filtered to produce an equation for $\bar{G}$, a quantity that is smoother than G. This equation contains, of course, terms representing effects of the scales that have been filtered out; these are the subgrid scale terms that must be represented by a model (Im 1995). In a simulation based on the filtered G-equation, the propagating flame is considered a contour of $\bar{G}$, which must propagate at a speed, $\bar{S}$, greater than the laminar flame speed; the increased speed plays the role of a subgrid scale model; alternative approaches to modeling will be discussed later. The filtered G-equation can then be written:

$$\frac{\partial \bar{G}}{\partial t} + \frac{\partial}{\partial x_j}(\bar{u}_j \bar{G}) = \bar{S} |\nabla \bar{G}|, \tag{4}$$

where

$$\bar{S}/S_L = 1 + C(u'/S_L), \tag{5}$$

and u' is the velocity fluctuation characterizing the unresolved scales and C is a constant that can be prescribed or calculated by the dynamic procedure. In an LES, u' must be modeled as well. However, as the present study is an initial investigation of modeling the G-equation, we shall calculate u' directly from the DNS velocity field. Likewise, the filtered velocity field, $\bar{u}_i$ is obtained directly from the DNS field. For later reference, we note that when the flame stretch and the Karlovitz number are not negligible, a diffusion-like term that represents the effect of stretch (Matalon & Matkowsky 1982) on flame propagation should be included on the RHS of Eq. (3) or (4).

3. A priori test of the flame area scaling law

We now present an *a priori* test of a dynamic subgrid-scale model for the turbulent flame speed; it is based on the model introduced by Bourlioux et al. (1996). Combining Eq. (1) and Eq. (5), we obtain the following equation:

$$\bar{S}/S_L = A_L/\bar{A} = 1 + C(u'/S_L), \tag{6}$$

where A_L is the flame area computed in a DNS, $\bar{A}$ is the filtered flame area to be computed in an LES, and $\bar{S}$ is the flame speed used in the LES. The latter was discussed above and should be selected to guarantee the correct overall burning rate, *i.e.* $\bar{S}\bar{A} = S_L A_L$. Eq. (6) is a useful subgrid-scale model if one can specify the model parameters appropriately. In this section, we first validate the linear relation, Eq. (6), and determine the constant C by using the resolved flame area A_L computed from the DNS results.

3.1 Test procedure

To check the validity of Eq. (6), we process the DNS databases in the following way.

1. Identify a flame surface in the DNS G-field and compute its area A_L by triangulation.

2. Filter the G and u obtained from the DNS database at various filter sizes (2Δ, 4Δ, ... are used, where Δ is the DNS mesh size).

3. For each filter, compute u' as the square root of the subgrid kinetic energy (*i.e.* the L_2 norm of the difference between the resolved DNS velocity field and the filtered field).

4. Given the filtered G-field, identify the 'filtered flame surface' and compute its area $\bar{A}$.

We then investigate the relationship between the ratio $A_L/\bar{A}$ and u' as a function of filter size.

3.2 Databases

We first consider premixed flames in homogeneous decaying turbulence (Trouvé & Poinsot 1994). In the flame, there is a smooth transition of the reaction progress variable, c, from 0 (fresh mixture) to 1 (burnt gas). We begin by defining a flame surface. Following Trouvé & Poinsot (1994), we choose the level surface with $c = 0.8$ as the flame front and define $G = c - 0.8$. Heat release effects are included in this DNS. Since the viscosity depends strongly on temperature, the turbulence intensity varies significantly across the flame so one must be careful when computing the turbulence intensity u'; the value on the unburnt side of the flame should be used. In practice, we obtain u' by taking a 2-D Fourier transform of the velocity field on cross-sections ahead of the flame, averaging over the unburnt side of the domain. Our tests show that the choice of averaging volume is not important as long as it is sufficiently far from the boundary.

The second data set is the result of DNS of the passive G-equation in forced isotropic turbulence (Im 1996). There is no heat release in this simulation. Several simplifications are used in the test procedure:

1. The G variable is available from the DNS and can be filtered for *a priori* tests.

2. In the absence of heat release, any contour of G can be considered a flame surface. The average front area can be computed from the volume average of $|\nabla G|$ (Kerstein *et al.* 1988).
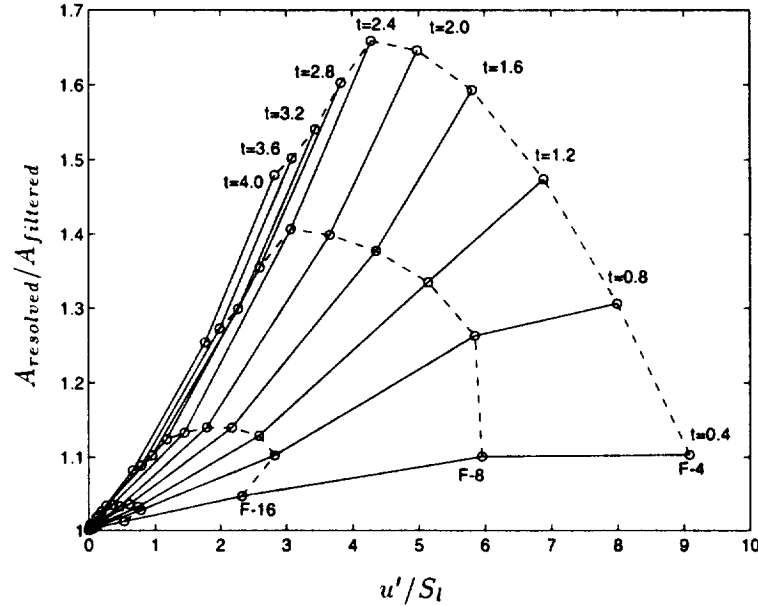
FIGURE 1. Ratio of the resolved DNS flame area to the filtered flame area as a function of the subgrid kinetic energy u'. DNS data by Trouvé & Poinsot (1994).

3. The entire flow field can be used to estimate u' - one does not need to distinguish the 'burnt' and 'unburnt' regions.

3.3 Results of the a priori test

Results of a priori tests applied to the database of Trouvé et al. (1994) are shown in Fig. 1. The ratio of the DNS flame area A_L to the filtered flame area $\bar{A}$ is plotted vs. the subgrid kinetic intensity u' at various times; the times shown are normalized by the large eddy turnover time. The DNS data were obtained on a 128^3 grid; each circle is a data point; the field was filtered to grids of 64^3, 32^3, 16^3 (F-16 on the figure), 8^3 (F-8) and 4^3 (F-4).

Figure 1 clearly shows that, if Eq. (6) is valid, its coefficient is strongly time dependent. There are two reasons for this. Firstly, the flame is initially planar and a few eddy turnover times are required to reach an 'equilibrium' state. Secondly, the turbulence is not forced; its decay can be seen from the decrease of the turbulence intensity at the coarsest filter size (F-4) with time. Nevertheless, the results do seem to indicate the existence of a universal relationship after the flame is sufficiently wrinkled; the change between times t=2.4 and t=4 is small compared to the change from t=0.4 to t=2.4. Even at large times, a distinction must be made between the behavior at small scales (the 64^3, 32^3, and 16^3 filters) and the large scales. The linear fit (6) appears reasonable for the small scales but not the large ones. This is an argument in favor of LES; modeling may be more universal for the small scales than for the large scales.

In the passive database (Im 1996), the flame front is again initially planar but,

after several turnover times, the flame area levels out. Plots of the inverse of the filtered flame area vs. the turbulent intensity are very similar to those found from the Trouvé/Poinsot database, with linear behavior for small values and quadratic behavior at larger scales.

We next test the dynamic procedure; it is based on the dynamic model for non-reactive flows. The parameter is adjusted using the smallest resolved scales of an LES. We shall not address the question of estimating u' but focus instead on estimating the subgrid flame wrinkling. Given $\bar{A}_1$ and $\bar{A}_2$, the flame area at filter sizes Δ_1 and Δ_2, and the corresponding subgrid turbulence intensities, u'_1 and u'_2, we use Eq. (6) to obtain:

$$A_L/\bar{A}_1 = 1 + Cu'_1,$$

$$A_L/\bar{A}_2 = 1 + Cu'_2.$$

This system can be solved to produce the resolved flame area A_L and/or the model constant C dynamically. Table 1 gives the results for the flame speed (characterized by $1/A_L$) obtained by applying the procedure described above to Im's data. The DNS field was filtered to 32^3 (F_1) and 16^3 (F_2) grids. The modeled turbulent speed is compared to the exact value obtained from the DNS. The agreement is excellent. There is little wrinkling on the small scales and the enhancement of the flame speed (the difference between turbulent and laminar speeds) is very small. The table also gives the error in the enhancement, which is acceptable. In the next section, we will describe attempts to incorporate this procedure into a dynamic LES.

Time	7.77	8.08	8.37	8.68	8.99	9.31
$\bar{S}_{dyn}$	1.0881	1.0598	1.0825	1.0887	1.1246	1.0706
$\bar{S}_{exact}$	1.0906	1.0633	1.0804	1.0801	1.1069	1.0672
E_1 (turbulent speed)	-0.7%	-0.3%	0.2%	0.8%	1.6 %	0.33 %
E_2 (enhanced speed)	-8%	-6%	3%	11%	16%	5%

Table 1. A priori test of a dynamical model for $\bar{S}$.

4. LES modeling test with spectral method

In this section, the SGS model presented in §2 is tested by applying it to flames in forced three-dimensional incompressible homogeneous isotropic turbulence; the simulations are carried out using a spectral method. Heat release is neglected in this test so the G-field behaves essentially as a passive scalar.

The calculation procedure is as follows. The flow field is fully resolved on a 64^3 grid using a pseudo-spectral method and second-order Runge-Kutta time-stepping (Rogallo 1981). The Reynolds number based on Taylor microscale is about 74. The turbulence is forced at the lowest wavenumber to maintain the kinetic energy constant. At every time step, the flow field is filtered onto a 32^3 grid; the resulting velocity field is then used in solving the filtered G-equation (4).
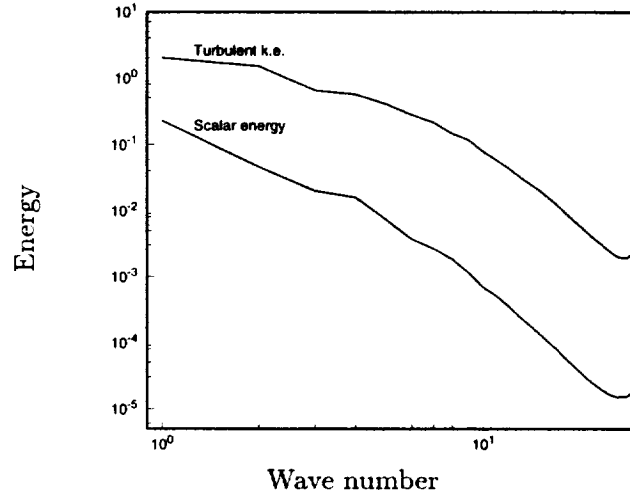
FIGURE 2.   Spectra of turbulent kinetic energy and scalar fluctuations in the 64^3 DNS calculation with $u'/S_L = 0.5$.

When the code was run with the model described above, numerical instability resulted. Investigation showed that the instability is due to an increase in the high wavenumber G-field, i.e., to cusp and strong gradient formation. It is necessary to do something to stabilize the calculation; one possibility is to add a second order diffusive term, $\mathcal{D}\nabla^2 G$, to the RHS of Eq. (4). As mentioned earler, similar terms are used to represent the effects of flame stretch and curvature on the flame speed. In the present DNS, $\mathcal{D}/\nu = 4$ is used where $\nu = 0.015$ is the molecular diffusivity.

Figure 2 shows the spectrum of turbulence kinetic energy and the scalar fluctuations, $\langle g^2 \rangle = \langle (G - \bar{G})^2 \rangle$ for $u'/S_L = 0.5$ obtained from the DNS. The turbulence was forced to allow attainment of steady state spectra in a few eddy-turnover times. We shall use this DNS field to construct the initial condition for the LES.

Specifically, the following subgrid-scale models are tested:

A. $\bar{S} = S_L$, i.e. no subgrid-scale model is used.

B. $\bar{S} = 1.08 S_L$, where the constant 1.08 was obtained from the a priori test.

C. $\bar{S}/S_L = 1 + 0.411(u'/S_L)$, a curve fit obtained from the a priori test similar to Fig. 1; u' is computed from the DNS flow field.

D. $\bar{S}/S_L = 1 + C(u'/S_L)$ with the parameter C computed dynamically by filtering the G-field to 16^3 resolution and assuming that the model $\hat{\bar{S}}/S_L = 1 + C(u'/S_L)$ applies at that level. The ratio $\hat{\bar{S}}/\bar{S}$ can be computed as the area of the constant G surface at the appropriate level of filtering.

The predictions produced by all these models are compared with results obtained by filtering the 64^3 DNS G-field. The Markstein diffusivity $\mathcal{D}$ used in all of the above LES was increased to twice the value used in the DNS to achieve stability. This can be interpreted as an extra subgrid-scale scalar transport required to represent the effects of the filtering. A more rigorous treatment of this term is necessary
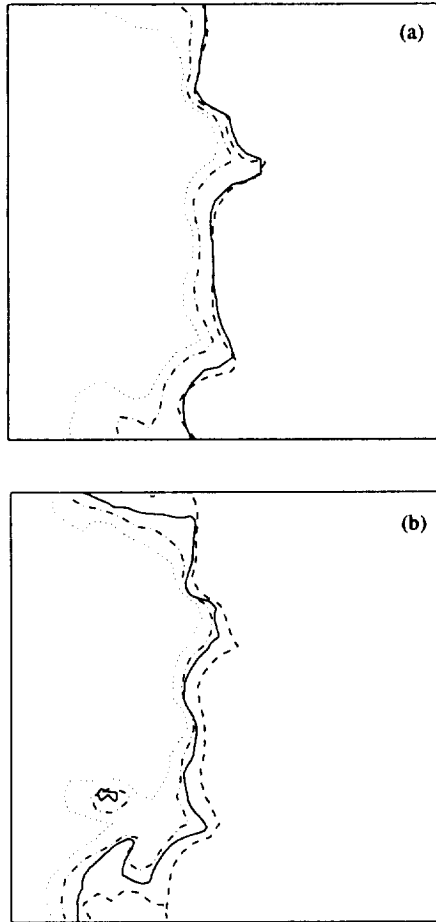
FIGURE 3. The contours of $\bar{G}$ obtained with various LES models after one eddy-turnover time; (a) $\bar{G} = 1.45$ which is the average value and (b) $\bar{G} = 1.95$. A single slice in 3-D is shown. In each figure, DNS result: ——— ; model A: – – – – ; model B: ⋯⋯⋯ ; model D: —·— . Flame propagates from right to left.

in the future; for example, a dynamic computation of $\mathcal{D}$ can be appended to the computation of C.

Figure 3 shows two $\bar{G}$ contours (1.45, 1.95) after one eddy turnover time for the various LES modeling strategies. Although the four fronts approximately reproduce the smoothed DNS contour, the various models give different average flame locations. It appears that model B overpredicts the turbulent flame speed, while model A underpredicts it, as expected.

The volume-averaged front location predicted by each LES model is compared to the DNS result in Fig. 4. All three LES models (B,C,D) overpredict the average flame speed. However, gradual improvement is obtained as the level of complexity of the model changes from the simple *a priori* procedure to the more sophisticated
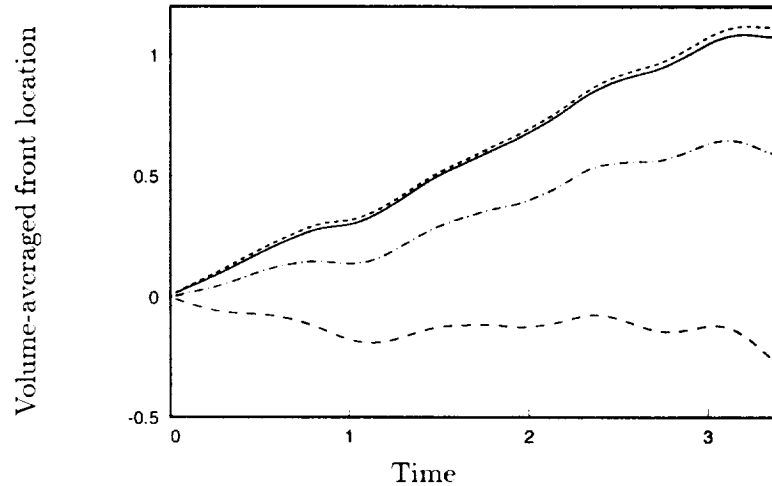
FIGURE 4.   The volume-averaged front location according to DNS and various LES models; model A: – – – – ; model B: ——— ; model C: ········· ; model D: —·— .

dynamic model. It is interesting to observe that, although model A underpredicts the flame speed, it gives the best agreement with the DNS.

It should be noted that the models used here are not complete. The supplementary subgrid-scale transport in the LES simulation was imposed by *ad hoc* adjustment of the diffusion coefficient, and was chosen mainly to achieve numerical stability of the spectral method. Improvement might be obtained by introducing a Smagorinsky-type model for the subgrid transport with model constant determined dynamically. This is currently being investigated.

5. Dynamic LES using a high order upwind scheme

The numerical stability issue addressed in §4 is easily understood by examination of Fig. 5 which gives several contours G at $t = 0.25$. The major cause of instability is the formation of cusps, which are present even at this early stage of the computation. Another difficulty is the squeezing together of contours, resulting in high gradients that are difficult to capture numerically. To address those difficulties, we repeated some of the experiments of §5 using a different solver for the G-equation, while retaining the spectral velocity field computation. The G-equation is now solved using a numerical strategy based on level-set technology (Osher & Sethian 1988, Sussman *et al.* 1994; for combustion applications Zhu & Sethian 1992, Klein 1995). For the advection term, we use a higher order upwind code developed by LeVeque (1993). The source term on the right hand side of Eq. (1) is solved with the procedure of Zhu & Sethian (1994). A reinitialization procedure is performed at every time step; the G-function is reinitialized to be the signed distance function with respect to the flame, using the procedure of Sussman *et al.* (1994). This means that only the $G = 0$ contour is considered to be a flame. Figure 6 displays contours obtained with this method; accuracy is maintained even when the flame becomes very distorted and no additional numerical viscosity needs to be added when the
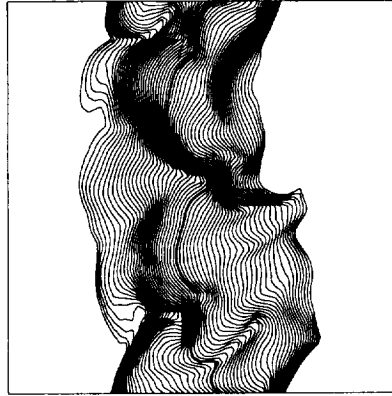
FIGURE 5.   Contours of the G function computed with spectral method. Flame propagates from right to left.
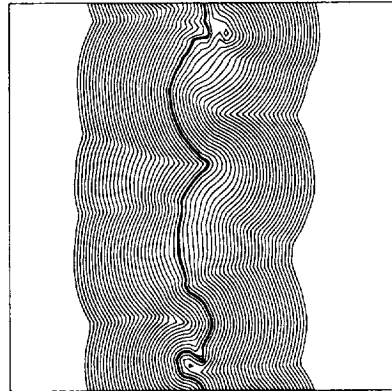

FIGURE 6.   Contours of the G function computed with higher order upwind method. Flame propagates from right to left.

mesh is coarsened. This method is roughly equivalent to introducing a viscosity or diffusivity selectively at those points at which the method of the preceding section had trouble, *i.e.* at cusps and in regions of large gradient of G.

In Fig. 7, we compare the results of a 32^3 computation with this procedure with the fully resolved 64^3 case results. The turbulent flame area is plotted as a function of time for different resolutions. The solid line is the 32^3 LES result, the dot-dash curve is the flame area in the 16^3 G-field obtained by filtering the 32^3 G-field. Using those data and the dynamic procedure of §3.3, the wrinkled flame area is extrapolated to the 64^3 grid (––––). This result is compared to the wrinkled flame area computed directly on a 64^3 grid (o). It is clear that the suggested procedure underestimates the flame wrinkling. To explain the difference, we also show the flame area on a 32^3 grid (□) and a 16^3 grid (▽) obtained by filtering the DNS data. The discrepancy between the LES and DNS results can be traced to two effects:
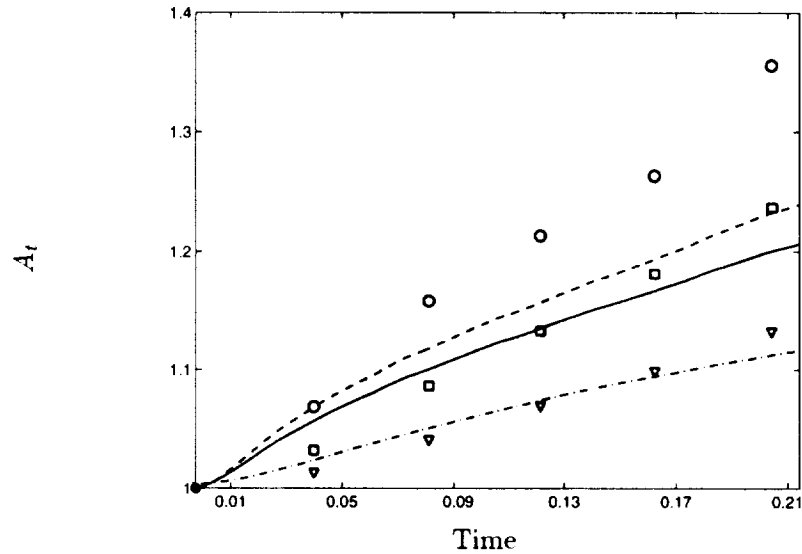
FIGURE 7.   Turbulent flame speed as a function of time from various DNS/LES calculations obtained with higher order upwind scheme. DNS results: 64^3, o ; 32^3, □ ; 16^3, ▽ . LES results: 64^3, - - - - ; 32^3, ——— ; 16^3, — · — .

- Underestimation of the flame area on the 32^3 grid: by comparing the 32^3 LES (———) and 32^3 filtered DNS (□) flame areas, it is clear that the upwind/reinitialization scheme smooths the wrinkled front slightly. This is to be expected from an upwind method - this effect is relatively small and could be controlled with a higher order method or a solution-adaptive integration procedure.
- Poor extrapolation of the subgrid wrinkling: extrapolation from the 32^3 and the 16^3 grids to the 64^3 grid magnifies the error which is relatively small on coarser grids; this is the major source of error.

This error can be better understood by looking at Fig. 8. In the computations, the linear fit (6) was used for dynamic extrapolation—the plot in Fig. 8 indicates that, in the early stages of flame wrinkling, the linear fit is inappropriate; a square root fit would be more suitable. This is consistent with the *a priori* test results reported in §3. Longer computations are being performed to assess whether this effect will disappear as the flame becomes sufficiently wrinkled.

6. Conclusions

Large eddy simulation will be necessary if reacting flows in complex geometries are to be simulated. This paper is a first attempt at evaluating models of subgrid scale effects that could be used in those flows. The laminar flamelet regime is considered in this paper such that the G-equation can be used as the basis for the modeling.

Since the effect of filtering is to smooth a wrinkled flame, a natural model is one in which the smoothed flame has a higher speed than that of the laminar flame. Simple models of this kind were constructed and tested using the *a priori* approach
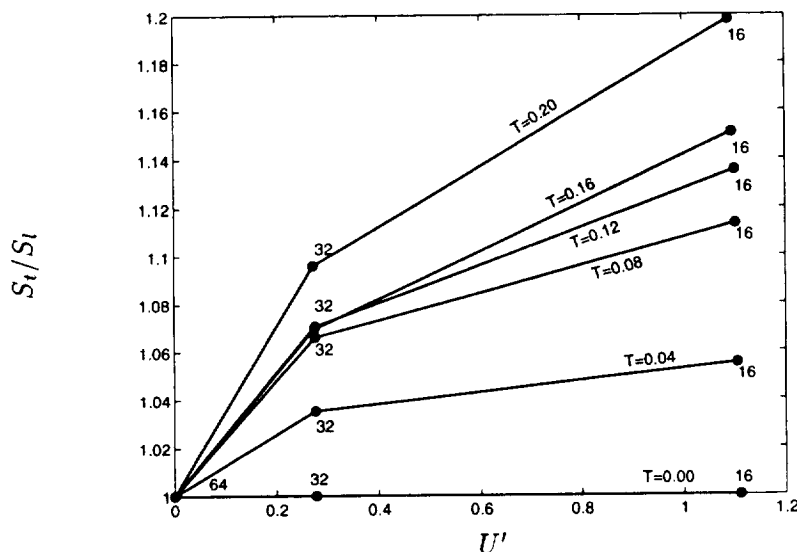
FIGURE 8.   Ratio of the resolved DNS flame area to the filtered flame area as a function of the subgrid kinetic energy u' at various filter levels. Results for passive G-field with higher order upwind method.

and large eddy simulations. *A priori* tests show that a linear relationship between the flame speed and the subgrid scale turbulent velocity is reasonable.

The models were then tested in two types of LES. In the first, the passive G-equation is solved along with the Navier–Stokes equations using a pseudo-spectral method. This approach is incapable of allowing heat release. Several versions of the model for the G-field were used including ones with a fixed constant and others with the parameter computed dynamically. These computations are numerically unstable, a problem that can be traced to the creation of cusps and high gradient regions. This problem can be eliminated through the addition of a diffusive term to the subgrid scale model. This can be justified in the same way that the Smagorinsky model is justified but, in this paper, the addition of the diffusive term was done in an *ad hoc* manner.

In the other type of LES, the G-equation is solved using a high order upwind method and the G-field is reinitialized at each time step. This approach essentially introduces diffusion where required to prevent the formation of cusps and high-gradient regions and requires no explicit diffusive terms.

The results show that the models are reasonable, but it appears that the LES models either overestimate (with a spectral method) or underestimate (with an upwind method) the turbulent flame speed. The reasons for this behavior are under investigation.

REFERENCES

BOURLIOUX, A., KLEIN, R. & MOSER, V. 1996 A dynamic subgrid scale model

for turbulent premixed flames. *CERCA* technical report.

CLAVIN, P. & WILLIAMS, F. A. 1979 Theory of premixed-flame propagation in large-scale turbulence. *J. Fluid Mech.* **90**, 589.

DAMKÖHLER, G. 1940 *Z. Elektrochem.* **46**, 601.

IM, H. G. 1995 Study of turbulent premixed flame propagation using a laminar flamelet model. *Annual Research Briefs-1995*, Center for Turbulence Research, NASA Ames/Stanford Univ.

IM, H. G. 1996 Large eddy simulation of turbulent premixed combustion using the G-equation model. *In preparation.*

KERSTEIN, A. R. & ASHURST, WM. T. 1992 Propagation rate of growing interfaces in stirred fluids. *Phys. Rev. Lett.* **68**, 934.

KERSTEIN, A. R., ASHURST, WM. T., & WILLIAMS, F. A. 1988 Field equation for interface propagation in an unsteady homogeneous flow field. *Phys. Rev. A.* **37**, 2728.

KLEIN, R. 1995 The level set approach to premixed turbulent combustion in the flamelet regime: theory and numerical implementation. Lecture Notes, *Euroconference on Premixed Combustion*, Aachen.

LEVEQUE, R. J. 1993 High-resolution conservative algorithms for advection in incompressible flow. *SIAM J. Num. An.* **33**, 627.

LIÑÁN, A. & WILLIAMS, F. A. 1993 *Fundamental aspects of combustion*, Oxford University Press.

MATALON, M. & MATKOWSKY, B. J. 1982 Flames as gasdynamic discontinuities. *J. Fluid Mech.* **124**, 239.

OSHER, S. & SETHIAN, J. A. 1988 Fronts propagating with curvature-dependent speed: algorithms based on Hamilton-Jacobi formulations. *J. Comp. Phys.* **79**, 12.

POCHEAU, A. 1992 Front propagation in a turbulent medium. *Europhysics Letters.* **20**, 401.

ROGALLO, R. 1981 Numerical experiments in homogeneous turbulence. *NASA TM81315.*

TROUVÉ, A. & POINSOT, T. 1994 The evolution equation for the flame surface density in turbulent premixed combustion. *J. Fluid Mech.* **278**, 1.

SUSSMAN, M., SMEREKA, P. & OSHER, S. 1994 A level set approach for computing solutions to incompressible two-phase flow. *J. Comp. Phys.* **114**, 146.

YAKHOT, V. 1988 Propagation velocity of premixed turbulent flames. *Comb. Sci. Tech.* **60**, 191.

ZHU, J. & SETHIAN, J. A. 1992 Projection methods coupled to level set interface techniques. *J. Comp. Phys.* **102**, 128.